

Altered Patterns of Gap Junction Distribution in Ischemic Heart Disease

An Immunohistochemical Study of Human Myocardium Using Laser Scanning Confocal Microscopy

Jonathan H. Smith,* Colin R. Green,*
Nicholas S. Peters,† Stephen Rothery,† and
Nicholas J. Severs†

From the Department of Anatomy and Developmental Biology,* University College London, and the Department of Cardiac Medicine,† National Heart and Lung Institute, London, United Kingdom

Arrhythmias are a common and potentially life-threatening complication of myocardial ischemia and infarction in humans. The structural pathways for the rapid intercellular conduction of the electrical impulse that stimulates coordinated contraction in the myocardium are formed by the gap junctions situated at intercalated disks. By raising antibodies to cardiac gap-junctional protein, and using these antibodies in an immunohistochemical procedure in combination with the technique of laser scanning confocal microscopy, we have succeeded in localizing gap junctions, with a clarity not previously possible, through thick volumes of human myocardial tissue. To explore the structural basis for ischemia and infarction-related arrhythmogenesis, antibody labeling and laser scanning confocal microscopy were applied to study the organization, distribution, and other characteristics of gap junctions in the explanted hearts of patients undergoing cardiac transplantation for advanced ischemic heart disease. In areas of myocardium free from histologically detectable structural damage, there was no significant difference in the size of distribution of labeled gap junctions, or in their number per intercalated disk, between left ventricular tissue (in which functional impairment was severe) and right ventricular tissue (in which functional impairment was minimal). However, in myocytes at the border of healed infarcts—zones to which the slow conduction responsi-

ble for reentry arrhythmias has been localized—the organization of gap junctions was markedly disordered; instead of being aggregated into discrete intercalated disks, gap-junctional immunostaining was spread extensively over myocyte surfaces. Some infarct zones were bridged by continuous strands of myocytes, coupled to one another by gap junctions, thereby linking healthy myocardium on either side. At their thinnest, these bridges were in some instances no wider than a single attenuated myocyte. The conclusions are 1) a widespread, generalized derangement of gap junction organization does not appear to underlie functional impairment in the ischemic heart, 2) a disorderly arrangement typifies gap junctions in myocytes of the infarct border zone, and this may contribute to alterations in conduction that are capable of precipitating reentry arrhythmias, and 3) delicate chains of myocytes traverse some healed infarcts, apparently forming electrically coupled bridges across what would otherwise constitute blocked zones. The weakest link in this chain can be a single, degenerating myocyte; avoidance of arrhythmia may therefore depend on the continued survival of this single cell. (Am J Pathol 1991, 139:801–821)

Cardiovascular disorders are the leading cause of premature death and disability in most western countries, and of this group of diseases, ischemic heart disease is the most prevalent. Abnormalities in the conduction and

Supported by grants from the Medical Research Council, British Heart Foundation, Wellcome Trust, and Royal Society. Dr. Colin Green is a Royal Society University Research Fellow.

Accepted for publication June 3, 1991.

Address reprint requests to Dr. Nicholas J. Severs, Department of Cardiac Medicine, National Heart and Lung Institute, Dovehouse Street, London SW3 6LY, UK.

propagation of the electrical impulse that stimulates cardiac contraction are frequently associated with myocardial ischemia and infarction, and resulting arrhythmias are believed to be directly responsible for more than half the deaths due to this disease.¹ Electrophysiologic studies have shown that a major cause of such arrhythmias involves circulating excitation and re-entry in the vicinity of the ischemic or infarcted zone.^{2,3} The low resistance pathways that allow the electrical impulse to flow rapidly and repeatedly between cardiac muscle cells, ensuring that their mechanical responses are orderly and synchronous in the healthy heart, are formed by gap junctions.⁴⁻⁶ In "working" myocardium, gap junctions are characteristically organized, together with fasciae adherentes and desmosomes, in discrete zones of interaction between adjacent plasma membranes called intercalated disks.^{4,6}

Gap junctions consist of aggregates of channels that span the plasma membranes of neighboring cells, linking their cytoplasmic compartments together. Apart from their role in transmission of the action potential between myocytes, gap junctions between cells in general permit the direct intercellular exchange of ions and small molecules (up to ~ 1 kDa), including those that regulate differentiation, tissue patterning, and development.^{7,8} The component channels of gap junctions are formed from pairs of connexons aligned with one another so as to bridge the narrow gap between the adjacent membranes. Each connexon consists of six subunits, each subunit being formed from a separate protein molecule.^{9,10} The gap-junctional proteins, termed connexins, are similar though not always identical in different tissues and species; so far, four distinct members of the "connexin family" have been identified in mammals, and further members have been reported in nonmammalian species.¹¹⁻¹⁷

The principal gap-junctional protein reported in the mammalian heart, as identified by molecular techniques, is a 43 kDa species, connexin43.^{17,18} From the predicted amino acid sequence of this molecule, we have recently raised a set of three polyclonal antibodies to the cardiac gap junction.^{19,20} These antibodies were raised to synthetic peptides that had been constructed to match different portions of the connexin43 molecule that were deduced to be situated on the cytoplasmic side of the membrane.^{17,19} By immunocytochemistry and Western blotting, we have confirmed that these antibodies bind specifically to cardiac myocyte gap-junctional proteins.²⁰ We have further showed that one of the antibodies in particular, when used for immunohistochemistry of fixed tissue in combination with laser scanning confocal microscopy, enables localization of individual gap junctions with greatly improved clarity, over more extensive vol-

umes of tissue, than has previously been possible.¹⁹ This has provided new opportunities for investigating the role of gap-junction distribution in relation to myocardial function in the normal and diseased heart.

The precise nature of the structural basis for the abnormalities in impulse-transmission pathways that lead to arrhythmogenesis in ischemia and infarction is unclear. The present study therefore set out to investigate, with the aid of antibody labeling and laser-scanning confocal microscopy, the organization, distribution, and other characteristics of gap junctions in the hearts of patients who have advanced ischemic heart disease.

Materials and Methods

Human Myocardial Tissue

The principal series of specimens comprised myocardial samples of left and right ventricle free wall (midregion), obtained from the explanted hearts of patients who were undergoing heart transplantation because of advanced ischemic heart disease. Five hearts, from male patients, aged 40–60 years, were studied. In addition, for comparison, samples of one heart from a female transplant patient (aged 47 years) who had primary pulmonary hypertension were obtained for study. Blocks of tissue, approximately 1 cm³, were excised from the freshly removed hearts of these transplant patients for fixation as described later. A second series of specimens was obtained after acquiring informed consent from three patients (males, aged 51, 54, and 60 years, all with three-vessel disease and previous infarction), who were undergoing coronary artery bypass grafting for arteriosclerotic coronary artery disease. Using isoflurane anesthesia and after establishment of right atrial/aortic cardiopulmonary bypass at 31°C, the ventricles were decompressed and the heart was stopped using ischemic arrest and fibrillation. Within 60 seconds of arrest, transmural biopsies were taken using a 14-gauge (1.5 mm specimen diameter) biopsy needle from the left ventricular apex and right ventricular free wall.

All specimens were immediately placed in Zamboni's fixation²¹ (2% paraformaldehyde, 0.2% picric acid, 0.1M phosphate-buffered saline, pH 7.4) for 2 to 6 hours. For the transplant material, fixation was carried out as soon as possible after removal of the heart. Because this could not be done in the operating theater, hearts were preserved using cold cardioplegia during transport to the laboratory. After fixation, all samples were washed in tap water, dehydrated in alcohol, placed in chloroform, and embedded in wax after standard histologic procedures.

Sections of all material were routinely examined by light microscopy after staining with hematoxylin and eosin.

Antibodies

The primary antiserum used to localize cardiac gap-junctional protein was raised against a synthetic peptide ("HJ") matching residues 131–142 of the 382 amino-acid cardiac gap-junctional protein, connexin43. These residues are believed to be exposed on the cytoplasmic side of and distant to the membrane.¹⁷ The antiserum was one of three produced in rabbits after crosslinking of the peptide to the carrier protein keyhole limpet hemocyanin. The two other antisera were to peptides "HH" and "HQ", corresponding to stretches of the connexin43 molecule closer to (or partially embedded within) the membrane.^{19,20} Screening was carried out by dot-blot assay, and specificity of the antibodies for gap-junctional proteins was confirmed by dot blotting and Western blotting.²⁰ That the antibodies bound to morphologically recognizable gap junctions was demonstrated in preparations of isolated cardiac gap junctions by cytochemistry at the electron microscopic level.²⁰

Immunolocalization

Sections (10 μm thick) of wax-embedded tissue were dewaxed in xylene, rehydrated through a graded ethanol series and washed in tap water. Incubation in a trypsin solution (containing 0.1% trypsin (Sigma), 0.1% CaCl_2 , 20mM Trizma base, pH 7.4) then followed for 10 minutes at room temperature to re-expose fixation-sensitive antigenic sites.²² The sections were washed with tap water and treated with 0.1 M L-lysine (as blocking agent) in phosphate-buffered saline containing 0.1% Triton X-100. Incubation with the primary antiserum (dilution 1:10 in phosphate-buffered saline) was carried out for 1 hour at 37°C. After washing with phosphate buffer, and secondary blocking with swine serum, secondary antibody treatment with swine anti-rabbit FITC (Dako; 1:20 dilution) was given for 1 hour in the dark at room temperature. After final washing in phosphate-buffered saline, the slides were mounted using Citifluor mounting medium (designed to reduce fading and autofluorescence). Immunostained sections were examined by conventional epifluorescence techniques using a Zeiss microscope, and by laser scanning confocal microscopy.

Laser-scanning Confocal Microscopy

For laser scanning confocal microscopy, immunolabeled sections were examined using a Bio-Rad Lasersharp

MRC-500. Gain and contrast levels were set according to procedures standardized to ensure that the image collected showed a full range of grey level values from black (0 pixel intensity level) to peak white (254 pixel intensity level). All sections were initially surveyed at low magnification at various levels so that overall patterns of gap junction distribution could be compared in cells oriented at different angles with respect to the section plane. From the immunostaining patterns seen in relation to the positions of the cells,²³ it was apparent that, in areas of myocardium showing minimal histopathologic alteration, gap-junction immunostaining reliably marks out the positions of the intercalated disks (see below). For more detailed study and data collection, representative samples of en face or near en face intercalated disks, recognized as characteristic groups of immunostained gap junctions, were collected at random from each tissue section. This was routinely done using a $\times 60$ (Nikon, NA 1.4) objective and the zoom 4 setting on the computer. A series of optical sections through each disk was taken at steps of 1 μm . These could be viewed individually, or projected together to reconstruct the intercalated disk, with its full complement of labeled gap junctions. Using the reconstructed disks from the transplant material, measurements of the longest dimension of the fluorescent spots representing gap junctions were made directly from the monitor using a mouse and the LEN (length) composite command in the standard software supplied. Corresponding measurements were made of spot size in border zone myocytes (which did not have gap junctions grouped into disks; see Results). From the reconstructions of disks of well-preserved myocardium, the number of junction spots per disk, and the area and longest dimension of each disk, were recorded. From these data, spot number per unit length of disk and per unit area of disk were calculated as comparative indices of junction frequency per disk. The measurements of area will inevitably underestimate the true areas of the intercalated disks, which, at the ultrastructural level^{4,6} are known to have a highly undulating topology. They do, however, represent valid comparative indices of area, and in contrast to data obtained by other techniques, are directly tied to accurate counts of the numbers of gap junctions over the entire area of the same disks. Longest axis of the disk was measured as an independent index of disk size to allow for the fact that some disks will not lie precisely at right angles to the direction of view, resulting in underestimation in the direct measurements of disk area. To examine whether the frequency of immunostained gap junctions varied according to overall size of the disk, data for three separate size classes of disk, selected to fall within the full range of disk sizes, were calculated. These size classes were designated small (defined as disks of

< 10 μm diameter), medium (disks of 10–20 μm diameter), and large (disks > 20 μm diameter).

Another potential source of error comes from the assumption that the full limits of an intercalated disk, which comprises the interacting plasma membrane domains of two neighboring cells and includes adherens junctions as well as gap junctions, will be revealed by gap junction immunostaining alone. Although some underestimation may arise from this source, three lines of evidence suggest that such an assumption does give a good approximation of overall disk size; 1) in longitudinally sectioned cells, the punctate immunofluorescent lines cross the full widths of cells and their bifurcations, 2) disks are characteristically bordered by a ring of large, particularly prominent immunostained junctions, and 3) disk dimensions measured by light microscopy of toluidene blue-stained resin sections are similar to those measured by confocal microscopy of immunostained sections. The abundance of immunostained gap junctions present, combined with the ability, by laser scanning confocal microscopy, to observe them through substantial depths of specimen, contributes to accurate delineation of the full extent of gap junction-containing regions of the disk.

Electron Microscopy

In addition to conventional histology and immunolabeling for confocal microscopy, some samples were also processed for electron microscopy. After transport to the laboratory in Zamboni's fixative, tissue pieces were subdivided under a dissecting microscope to provide matching samples for electron microscopy and histologic processing. The former samples were transferred to 2.5% glutaraldehyde in 0.1 M sodium cacodylate buffer, pH 7.3; the latter were returned to Zamboni's fixative. The shapes of each divided specimen was recorded so that the matching cut surfaces could subsequently be identified and sectioned by both techniques to facilitate correlation between electron microscopy, high-resolution light microscopy of resin sections, standard histology of wax sections, and laser scanning confocal microscopy. After 2 hours of fixation in glutaraldehyde, specimens destined for electron microscopy were rinsed in cacodylate buffer, postfixed in 2% osmium tetroxide (cacodylate-buffered) for 2 hours, rinsed in 30% then 50% ethanol, and *en bloc* stained with uranyl acetate (saturated solution in 50% ethanol). Dehydration continued in an ethanol series, before embedding in epoxy resin. Ultrathin sections were stained in uranyl acetate and lead citrate, and examined in a Philips EM 301 electron microscope. Semithin sections for light microscopy, stained with 1% toluidene blue in a solution of 1% borax/50% ethanol, were routinely prepared in parallel.

Results

Histology and General Ultrastructure

The histopathology of all hearts was routinely assessed by examination of hematoxylin and eosin-stained wax sections. Large healed infarcts were readily identified as extensive, conspicuous areas of fibrosis (Figure 1a); smaller healed infarcts (< 500 μm diameter), and areas of more generalized fibrosis were common findings in the ischemic hearts. Nevertheless, many areas of myocardium distant from healed infarcts showed an orderly arrangement of fibers and an overall cellular structure resembling that of normal myocardium. This is illustrated in Figure 1b, which shows a toluidene blue-stained resin section taken from subepicardial myocardium in the region of the subendocardial infarction illustrated in Figure 1a. By high-magnification inspection of such sections, myocytes in these well-preserved zones appeared to be connected to one another by intercalated disks of normal structure as judged by light microscopy (Figure 1c).

In contrast to these structurally well-preserved myocytes, evidence of degenerative change was common in patches of myocytes immediately adjacent to or projecting into healed infarcts. The principal changes detectable in these cells by light microscopy were disarray of myocyte orientation, reduction of myofibrillar content with clearing of cytoplasm, alteration of cell shape to rounded or attenuated forms, and in occasional cells, enlarged or multiple nuclei (Figure 2a). Thin-section electron microscopy showed that myofibrillar disorganization was widespread. In myofibrils that were essentially intact, the individual myofilaments, instead of following a straight course, were often arranged in a parallel zig-zag or undulating fashion (Figure 2b). Elsewhere, evidence for disintegration of the myofibrils and their component myofilaments, associated with the appearance of granular (myofibril-free) peripheral patches of cytoplasm, was frequently encountered (Figure 2c). The extent of these changes varied considerably in different cells.

Immunohistochemistry of Gap Junctions by Conventional Light Microscopy

Immunolocalization of gap junctions by standard epifluorescence light microscopy using "HJ" antiserum gave reproducible and consistent staining patterns, common to left and right ventricle. In areas of well-preserved myocardium, distant from healed infarcts (corresponding to those illustrated in Figure 1b, c), gap junctions were visualized as aggregates of bright green fluorescent domains, marking the positions of intercalated disks between myocytes. In longitudinally sectioned myofibers,

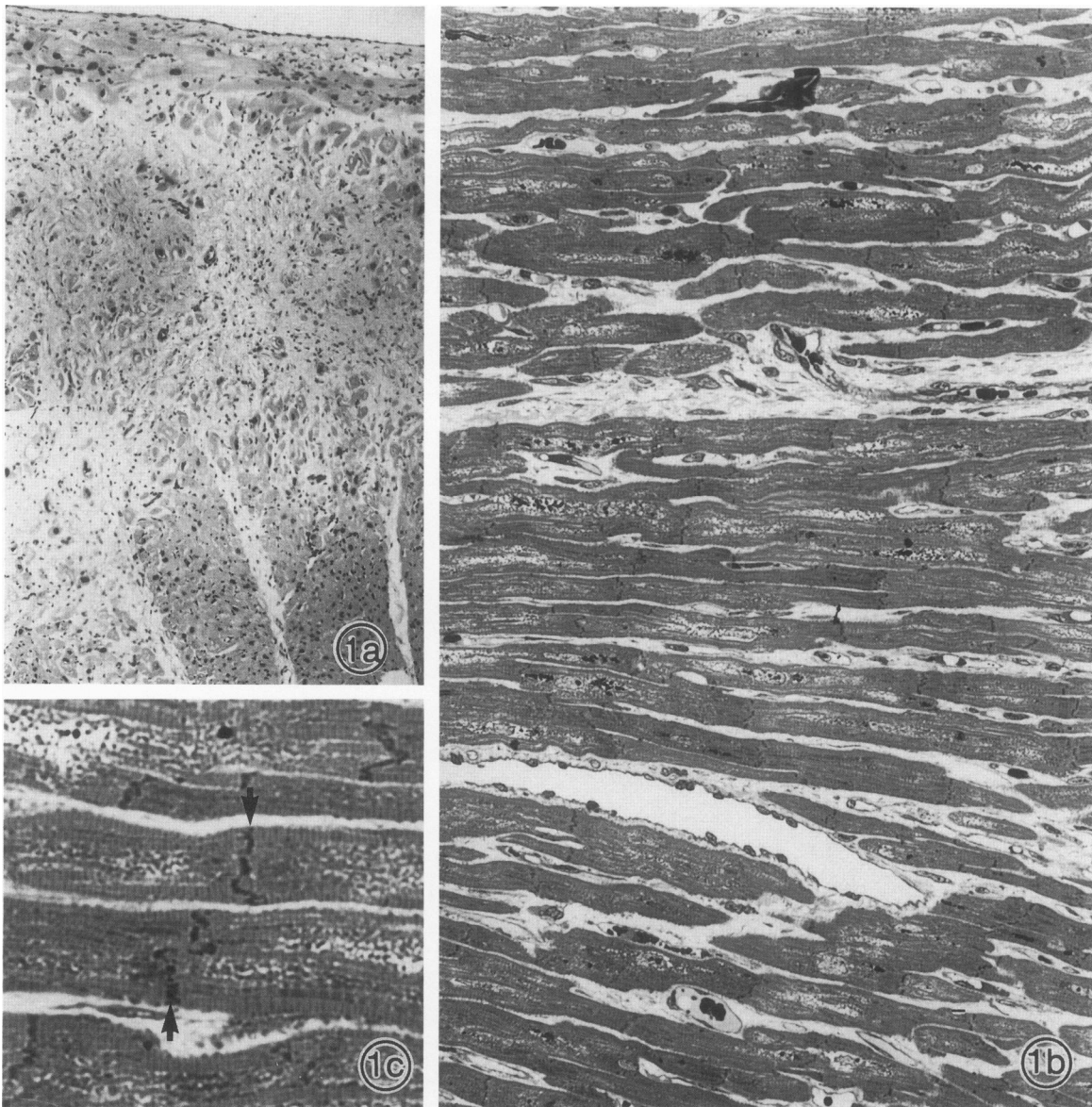


Figure 1. Typical light microscopic features of the left ventricular myocardium of a patient undergoing transplantation for advanced ischemic heart disease. **a:** Standard H & E wax section showing survey view of a subendocardial infarct. **b:** Detail of structurally well-preserved myocardium, taken from subepicardial myocardium in the same region, viewed in a toluidene blue-stained resin section. Note that the myocytes are well aligned and show no visible abnormalities in structure. **c:** Higher magnification detail of well-preserved myocytes like those in (b) shows intercalated disks (arrows) running transversely across the long axis of the myocytes in the manner characteristic of normal myocardium, **a**, $\times 71$; **b**, $\times 285$; **c**, $\times 900$.

where the disks are viewed edge-on, the individual domains tended to merge, giving the disks the appearance of sets of short, transversely oriented lines (Figure 3a). Where sections were cut transversely with respect to the long axis of the fiber, allowing viewing of the intercalated disks face-on, individual spotlike junctions were more easily discriminated (Figure 3b). Here, the disks were typically outlined by a peripheral ring of prominent staining, circumscribing an interior region containing numerous less prominent spots. Obliquely sectioned myocytes showed intermediate, foreshortened views of the disk.

Controls in which "HJ" antiserum treatment was omitted or substituted with pre-immune serum showed no fluorescent labeling. When immunolocalization was attempted on fixed tissue-sections with antiserum to peptides "HH" and "HQ," no staining of the disks was observed, though under appropriate conditions, these antisera do give comparable staining patterns on cryosections. Although the immunostaining procedure using "HJ" gave a strong signal for myocyte gap junctions, no immunostaining of nonmyocyte cell types (interstitial fibroblasts, valve myofibroblasts, and vascular

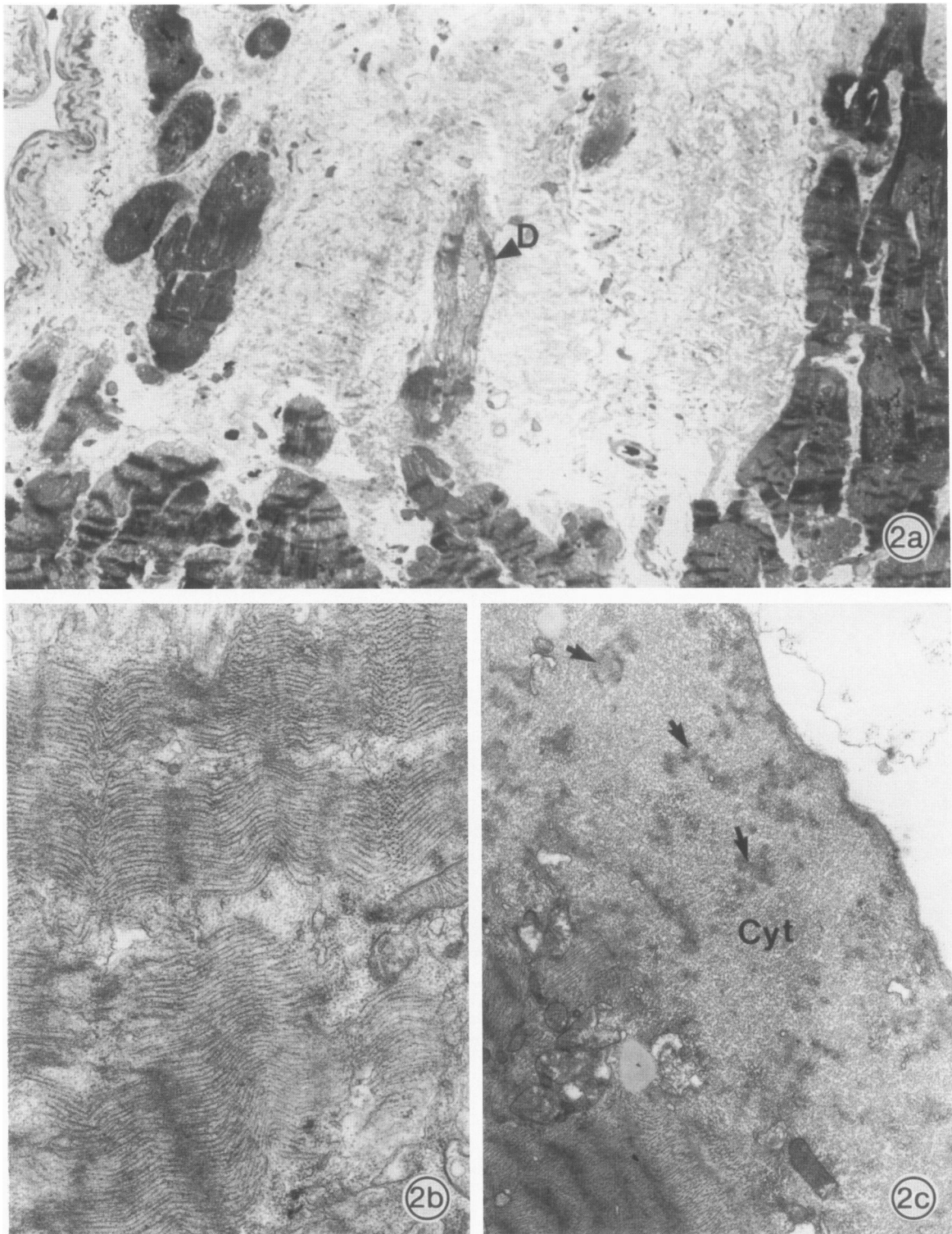


Figure 2. Typical structural features of myocytes in the border region of a healed infarct (from a needle biopsy of left ventricular myocardium taken from a patient undergoing coronary bypass surgery). **a:** light microscope view of a toluidene blue-stained resin section, illustrating myocytes adjacent to and penetrating within the healed infarct zone. Highly abnormal degenerating myocytes (**D**), with a dearth of contractile apparatus, are present. The contracture bands in the surrounding myocytes may in part be a pathologic feature, but occur widely throughout myocardium that is obtained by needle biopsy; **(b)** and **(c)** are thin section electron micrographs from myocytes to the top left of the field in **(a)**, illustrating abnormal features of myofibril organization in these cells. In **(b)** the myofibrils are essentially intact, but their component myofilaments are arranged in undulating fashion. **(c)** shows a peripheral area of myofibril-free cytoplasm (**cyt**), a common feature of border zone cells. These areas appear where the myofibrils disintegrate. The darkly staining patches in this zone (arrows) represent remnants of disintegrated myofibrils. **a**, $\times 285$; **b**, $\times 20,500$; **c**, $\times 13,500$.

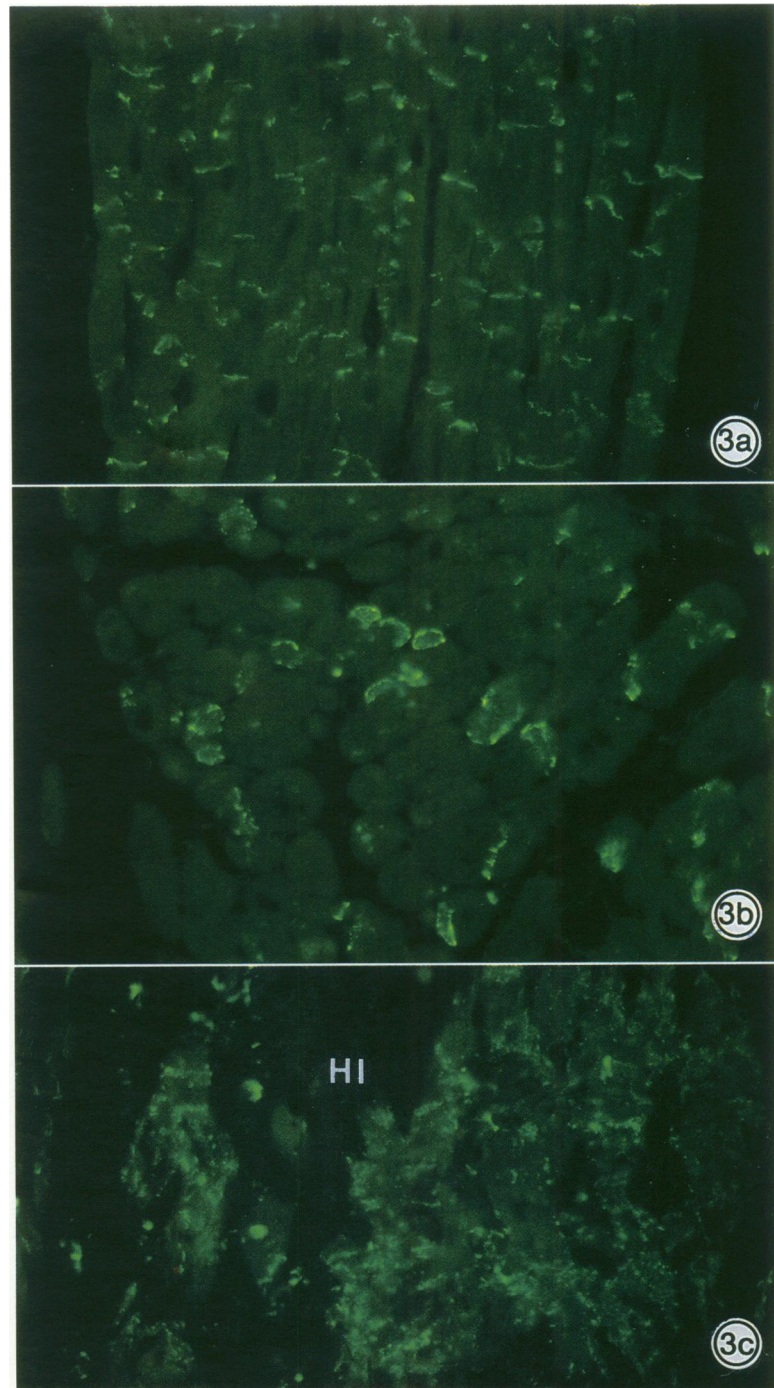


Figure 3. Immunolocalization of gap junctions in human heart, as viewed by conventional fluorescence light microscopy (left ventricle, transplant patient). **a:** Longitudinally sectioned myofiber from histologically well-preserved myocardium. Staining of the gap junctions shows the intercalated disks as short, bright green lines, running at right angles to the long axis of the cells. **b:** Sections through well-preserved myocardium cut transversely with respect to the long axis of the cells. The intercalated disks are viewed face-on, and some individual junctions can just be resolved as single fluorescent spots. **c:** Myocardium adjacent to a healed infarct (HI). The pattern of gap junction distribution differs markedly from that of the well-preserved myocardium in (a) and (b). Instead of being confirmed to well-defined intercalated disks, the immunostained gap junctions appear widely dispersed over the cells, $\times 184$.

smooth muscle cells) was detectable. A high level of autofluorescence was apparent in vascular smooth muscle.

Healed infarct zones were readily identified in the "HJ" antiserum-stained sections. They showed no immunostaining of gap junctions, but often contained grapelike

clusters of autofluorescing material, due to lipofuscin or remnants of nuclei. Myocytes bordering infarcts showed positive staining for gap junctions, but in contrast to more distant myocardium, the fluorescent label often appeared distributed in a more disorderly fashion over the cell (Figure 3c).

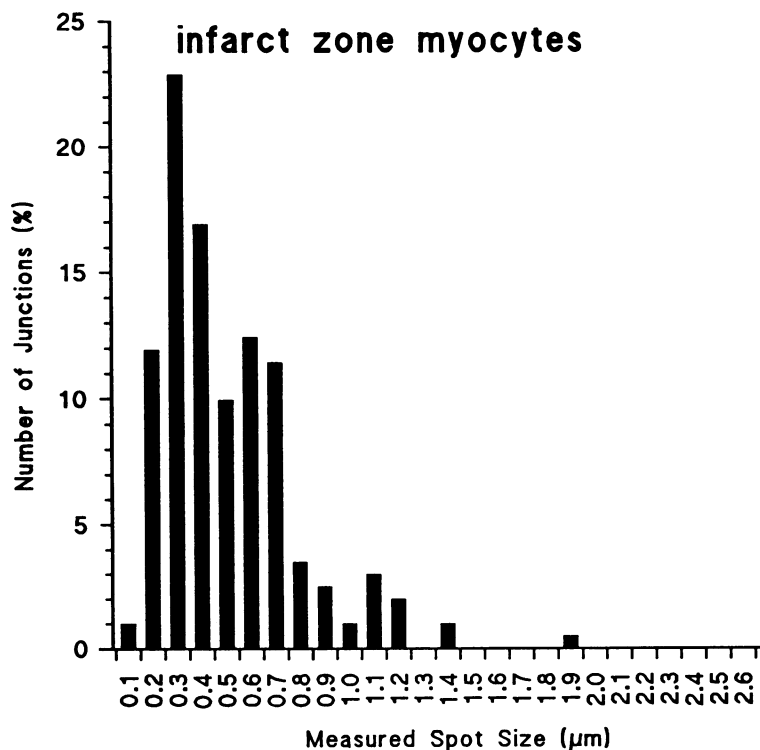
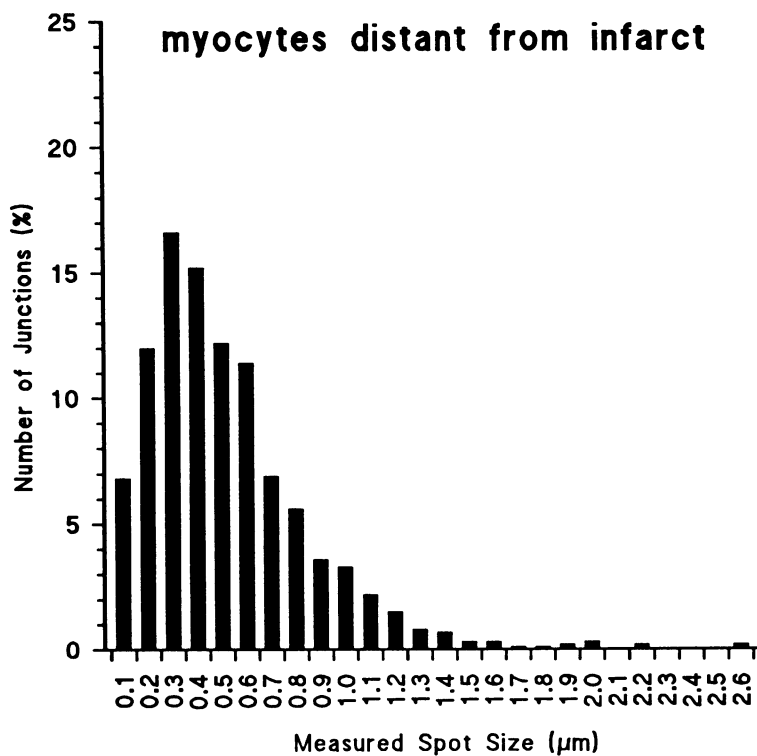


Figure 4. a: Data on size of labeled gap junctions visualized by laser scanning confocal microscopy in human ventricular myocardium; This figure shows the frequency distributions of the diameters of the fluorescent spots marking the junctions in myocytes distant from the healed infarct and in infarct border zone myocytes.

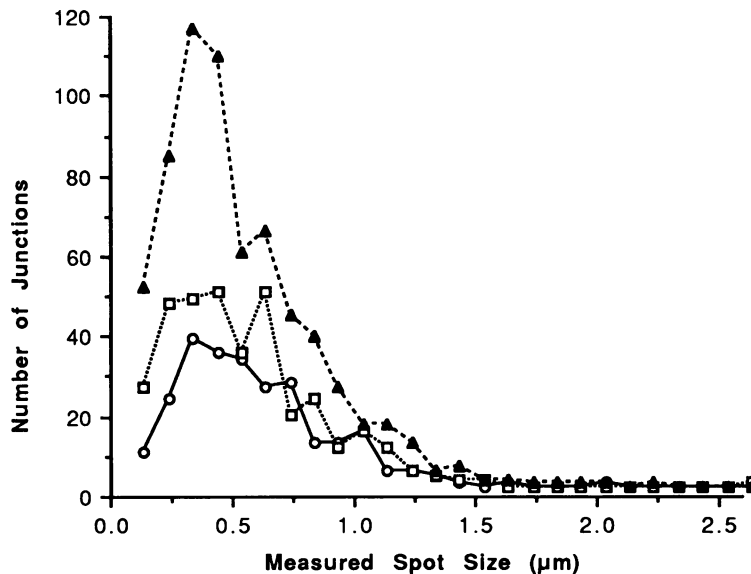


Figure 4. b: This figure shows the frequency distributions of the fluorescent spot diameters in intercalated disks of different size. \circ , disks $< 10 \mu\text{m}$; \square , disks $10\text{--}20 \mu\text{m}$; \blacktriangle , disks $> 20 \mu\text{m}$. Note that the stained gap junctions are of similar dimensions, irrespective of the size of the intercalated disks. (Data taken from a total of 1255 junctions).

Immunohistochemistry of Gap Junctions by Laser Scanning Confocal Microscopy

By using laser scanning confocal microscopy to examine sections stained with "HJ" antiserum, a marked improvement in the clarity of gap junction localization was possible. This allowed 1) collection of quantitative data on labeled gap junctions in left and right ventricular myocardium, and 2) detailed comparison of gap junction distribution in areas bordering healed infarcts with that in more distant myocardium.

Gap junction size, as measured by fluorescent spot diameter in the laser scanning confocal microscope, showed no significant difference between the structurally well-preserved areas of left and right ventricular myocardium in the ischemic hearts. Left and right ventricular myocardium in the patient who had pulmonary hypertension gave similar results. As shown in Figure 4a, the frequency distribution of labeled gap junction size obtained from the pooled results on structurally well-preserved myocardium did not differ from that of border zone myocytes. The mean diameter of the labeled junctions was determined as $0.513 \mu\text{m}$, and the modal value was $0.3 \mu\text{m}$. Measurements of the fluorescent spot diameter in small ($< 10 \mu\text{m}$ diameter), medium ($10\text{--}20 \mu\text{m}$ diameter) and large ($> 20 \mu\text{m}$) intercalated disks indicated that the gap junction size distribution did not vary with the size of the disk (Figure 4b). Gap junction density, as measured by spot number per unit length of disk long axis and by spot number per unit area of en face disk, also showed no differences between the samples, and appeared to remain approximately constant in disks of different sizes

(Figure 5). The mean number of gap junction spots per $1 \mu\text{m}$ disk long axis was 5.34 ± 2.03 , and the mean number of spots per unit area of disk viewed face-on was $0.69 \pm 0.27 \mu\text{m}^{-2}$.

The basic pattern of gap junction staining observed by conventional epifluorescence was confirmed with striking clarity by laser scanning confocal microscopy (Figure 6). The definition of detail was such that a much clearer picture of gap junction organization at the disk became possible (Figures 6, 7). In longitudinally sectioned cells, the lines of staining marking the disk are resolved as series of separate spots (Figure 6a). These punctate lines of staining often extend across the full widths of the end-on abutments between cells; shorter punctate lines occur at connections between bifurcations of the main cell bodies. Viewed face-on, the border of the typical intercalated disk is delineated in an irregular, discontinuous manner by a series of large, sharply defined brightly staining gap junctions that vary in shape from round to irregular or elongate (Figures 6b, 7). In their longest dimension, the fluorescent patches marking these junctions measure up to $2.6 \mu\text{m}$. The gap junctions in the interior zone of the disk are seen as smaller but distinct domains down to $0.1 \mu\text{m}$ in diameter. They are rounded, and although some fluoresce just as brightly as the large peripheral junctional domains, others—of apparently similar size—appear fainter and less clearly defined.

The gap junction staining patterns of myocytes in the border zones of healed infarcts were different from those observed elsewhere (Figure 8). In these zones, the fluorescent staining was often no longer confined to the well-

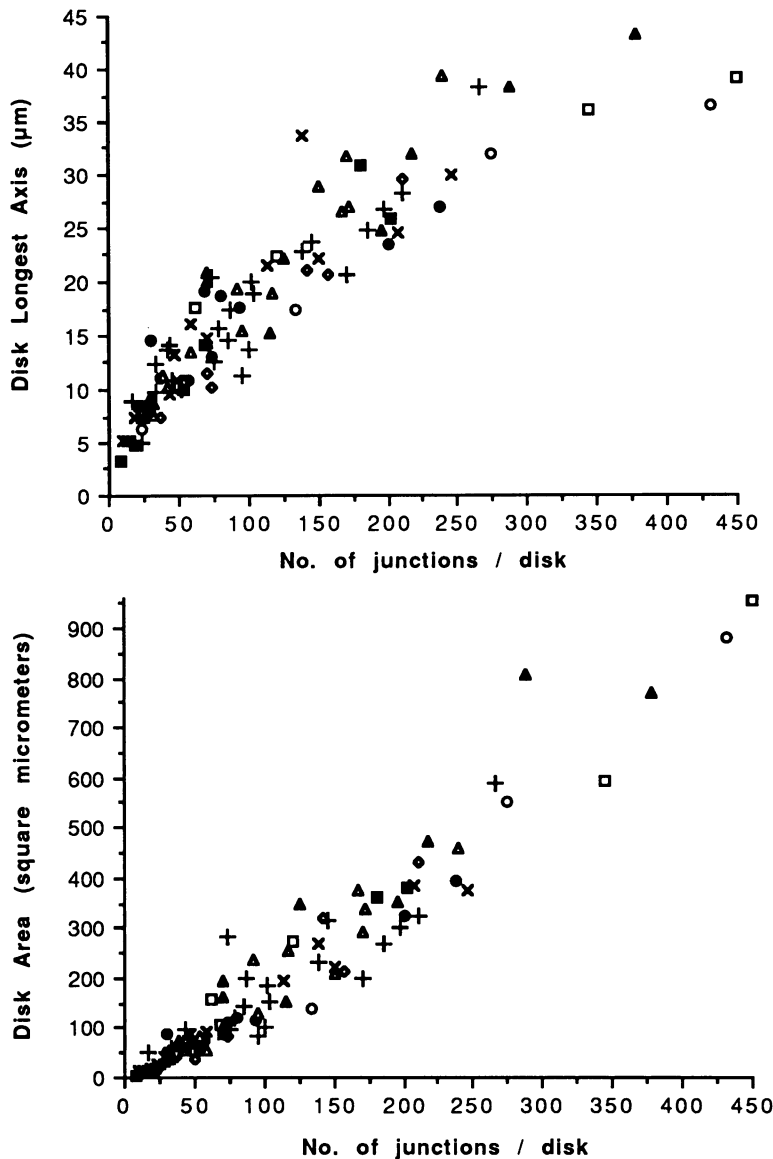


Figure 5. Data on numerical density of gap junctions, as measured by number of fluorescent spots per unit length of the longest diameter of the disk (a), and number of spots per unit area of the disk (b). Note that because of the highly folded topology of the disk, the measured areas in (b) will underestimate the true area; both types of measurement nevertheless provide reliable comparative indices. Note that the numerical density of gap junctions in intercalated disks is approximately constant in intercalated disks of different size. Each symbol represents a different heart.

defined foci representing normal intercalated disks. Instead, the pattern of fluorescence showed varying degrees of dispersion over the cell surface. Although this was minimal, it was still possible to identify the approximate position of the intercalated disk by the presence of aggregates of labeled junctions, though the organization as a prominent ring enclosing small spots was no longer discernible (Figure 8b, d). In many instances, however, a recognizable intercalated disk could no longer be seen (Figure 8a,c). In some views, the labeled junctions appeared to lie within rather than at the surface of a cell, but serial optical sectioning showed that such junctions were situated at areas of close juxtaposition between two cells (Figure 9). The altered staining patterns were generally confined to a depth of the first five layers of myocytes surrounding the infarct. Staining was seldom present

along the surfaces of myocytes facing the healed infarct (Figure 8b, d). Overall, the disordered patterns of gap-junction immunostaining tended to become more pronounced as the size of the infarct and the histologic abnormality of its surrounding myocytes increased. There were exceptions to this trend, however, particularly in myocytes associated with smaller areas of fibrosis (e.g., those similar to Figure 8b). In some instances, these showed normal intercalated disk-patterns of gap junction immunostaining, whereas in others, markedly disordered patterns were apparent.

A noteworthy feature of some infarct zones was the presence of "peninsulas" and bridges comprising intact, interacting myocytes, projecting into or completely across the areas of fibrosis (Figure 10). "Peninsulas" frequently showed gap-junction fluorescence at their tip, in-

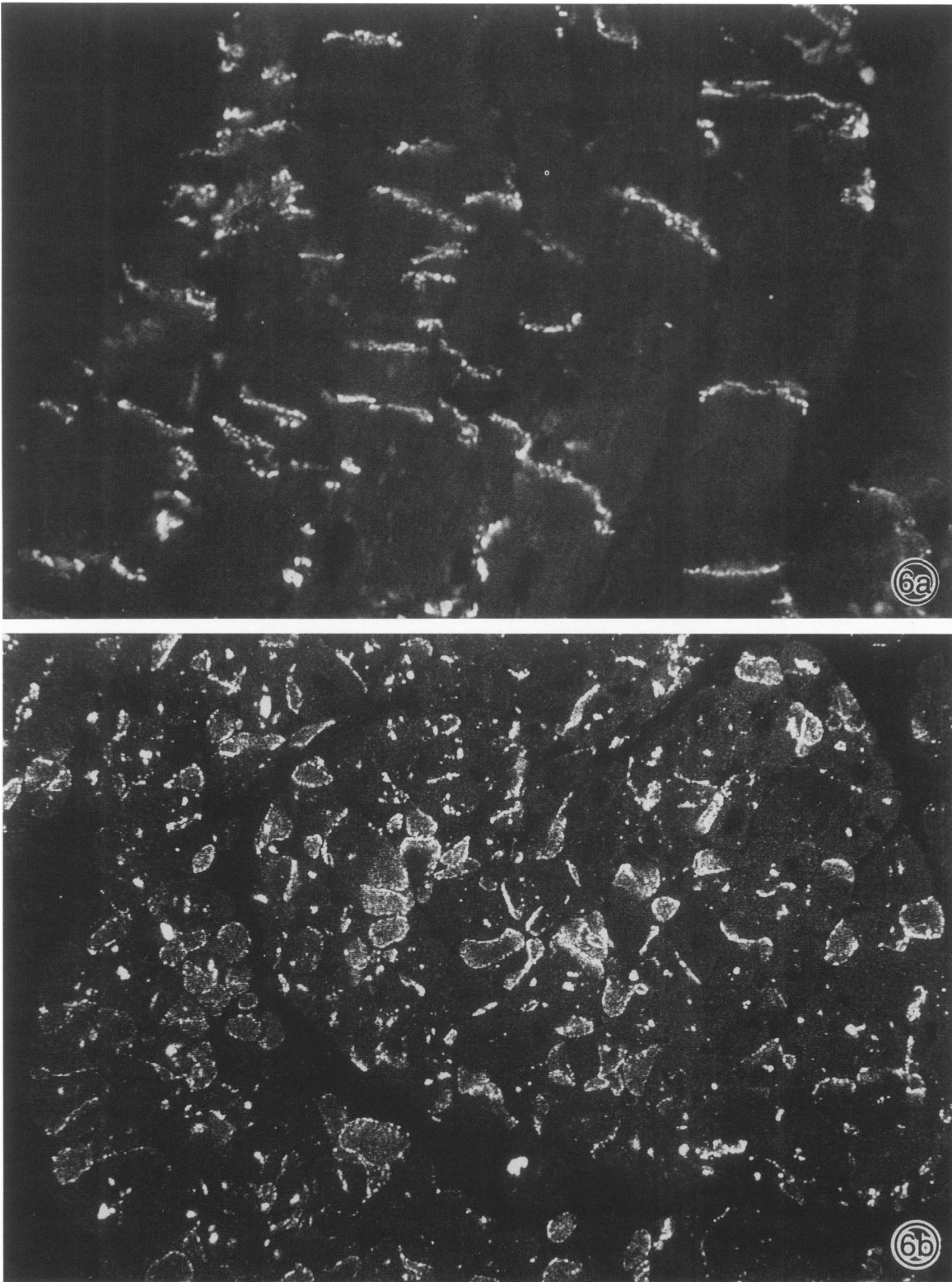


Figure 6. Immunostained gap junctions from human ventricle as observed by laser scanning confocal microscopy (left ventricle, transplant patient). The example in (a) is from a single optical section of a tissue slice cut longitudinally with respect to the long axis of the myocytes; (b) is a survey view of transversely sectioned cells, reconstructed from multiple optical sections. The distribution of gap junctions is similar to that seen by conventional fluorescence microscopy (Figures 1, 2), but the ability to discriminate individual junctions is greatly improved. When the immunostaining pattern is examined in relation to the positions of the cells, which are just visible as "ghostlike" images, it can be seen that the gap-junction immunostaining patterns correspond closely to, and can be used as markers for, the intercalated disk as a whole. a, $\times 513$; b, $\times 260$.

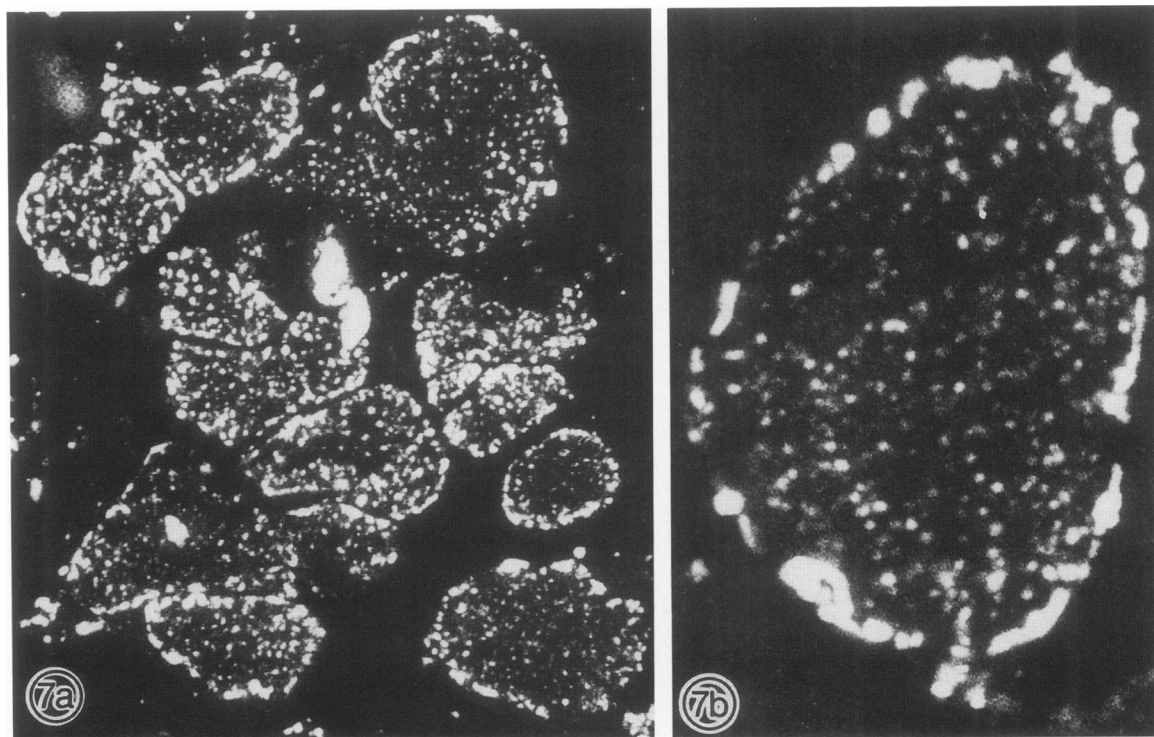


Figure 7. Higher magnification views of immunostained gap junctions in disks viewed face-on in the laser scanning confocal microscope (i.e., sections cut transversely across the myofiber, as in Figure 6b). The larger, and most brightly staining fluorescent spots tend to be located at the periphery of the disk, with numerous, smaller spots in the interior zone; (a) is a projection of $15 \times 1 \mu\text{m}$ sections; (b) is a projection of $13 \times 1 \mu\text{m}$ optical sections. a, $\times 416$; b, $\times 3340$.

dicating that contact of the apparently terminal myocyte continued with further myocytes out of the plane of section (Figure 10c). In some instances, chains of myocytes could be traced linking healthy myocardium on either side of the infarct (Figure 10a). The component myocytes of these chains were typically thin and attenuated, and had a reduced myofibril content. At their thinnest, the width of these bridges comprised a single elongated myocyte that contacted neighboring myocytes towards either end. Gap junction staining at such contact points was commonly detected. The interaction between myocytes in these bridges was predominantly mediated by dispersed, often laterally disposed gap junctions, though discrete intercalated disks were also identifiable, especially as the bridges approached healthy myocardium (Figure 10b, c).

Ultrastructural Correlates of Altered Immunostained Gap-junction Distribution

To investigate the ultrastructural basis for the observed alterations in distribution pattern of immunostained gap junctions, the intercalated disks and junctions of border zone myocytes were studied in further detail by thin section electron microscopy. Myocytes showing minimal de-

generative change frequently possessed intercalated disks of normal structure, with transversely-oriented plicate regions containing fasciae adherentes, and gap junctions situated in segments of the disk lying at right angles to these, parallel with the long axis of the cell (Figure 11a, b). However, disks in which this regular geometry had been lost were not uncommon, especially in cells that showed abnormally arranged contractile elements (Figure 11c, d). In some of these disks, the intercellular junctions remained grouped together, but the disk appeared as an irregular meandering structure between the cells (Figure 11c). In others, groups of junctions appeared to have become displaced from one another (Figure 11d). Separation of the membranes of the disk was found between some cells, though gap-junctional contact between such cells was maintained elsewhere (Figure 11e).

The diverse changes in overall architecture of the disk appear to be the outcome of alterations in cell shape, disorganization of the contractile apparatus and other degenerative change in infarct zone myocytes. In the course of this remodelling process, gap-junctional membrane appears frequently to become displaced from its usual location so that it is no longer found exclusively in association with adherens junctions. Examples of such gap junctions, which characteristically have highly con-

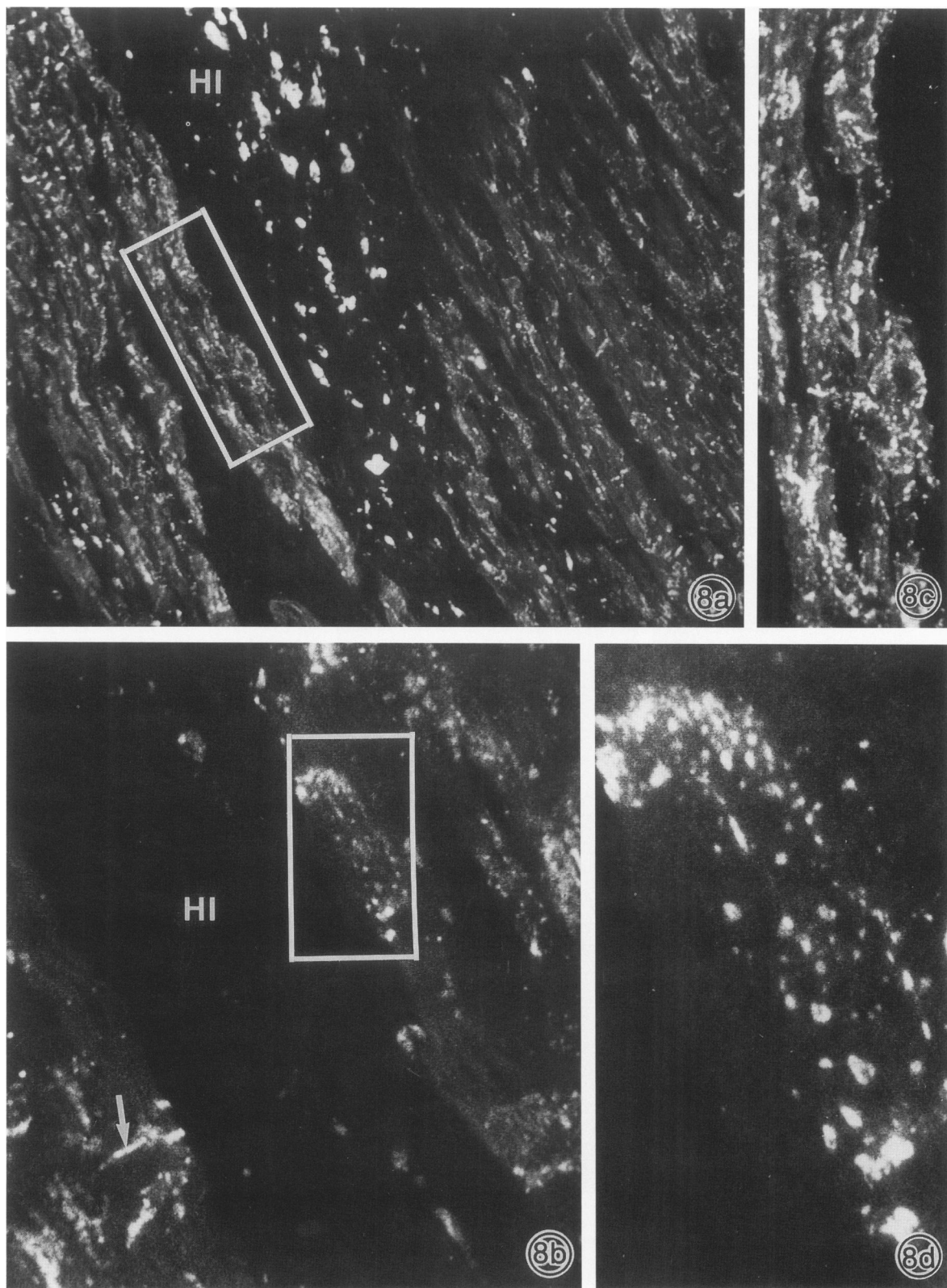


Figure 8. Gap junction distribution in myocytes bordering healed infarcts, as viewed by immunostaining and laser scanning confocal microscopy (left ventricle, transplant patient). Fields (a) and (b) show low magnification views; enlargements of the boxed areas are shown in (c) and (d), respectively. Note that border zone gap junctions appear widely dispersed. The normal segregation of gap junctions into intercalated disks is nevertheless retained by some cells, arrow, panel (b). Note that the irregular white patches within the healed infarct (HI) are due to autofluorescence, not the presence of gap junctions; (a) and (c) are composite images prepared from multiple optical sections; (b) and (d) are from single optical sections. a, $\times 143$; b, $\times 780$; c, $\times 355$; d, $\times 2520$.

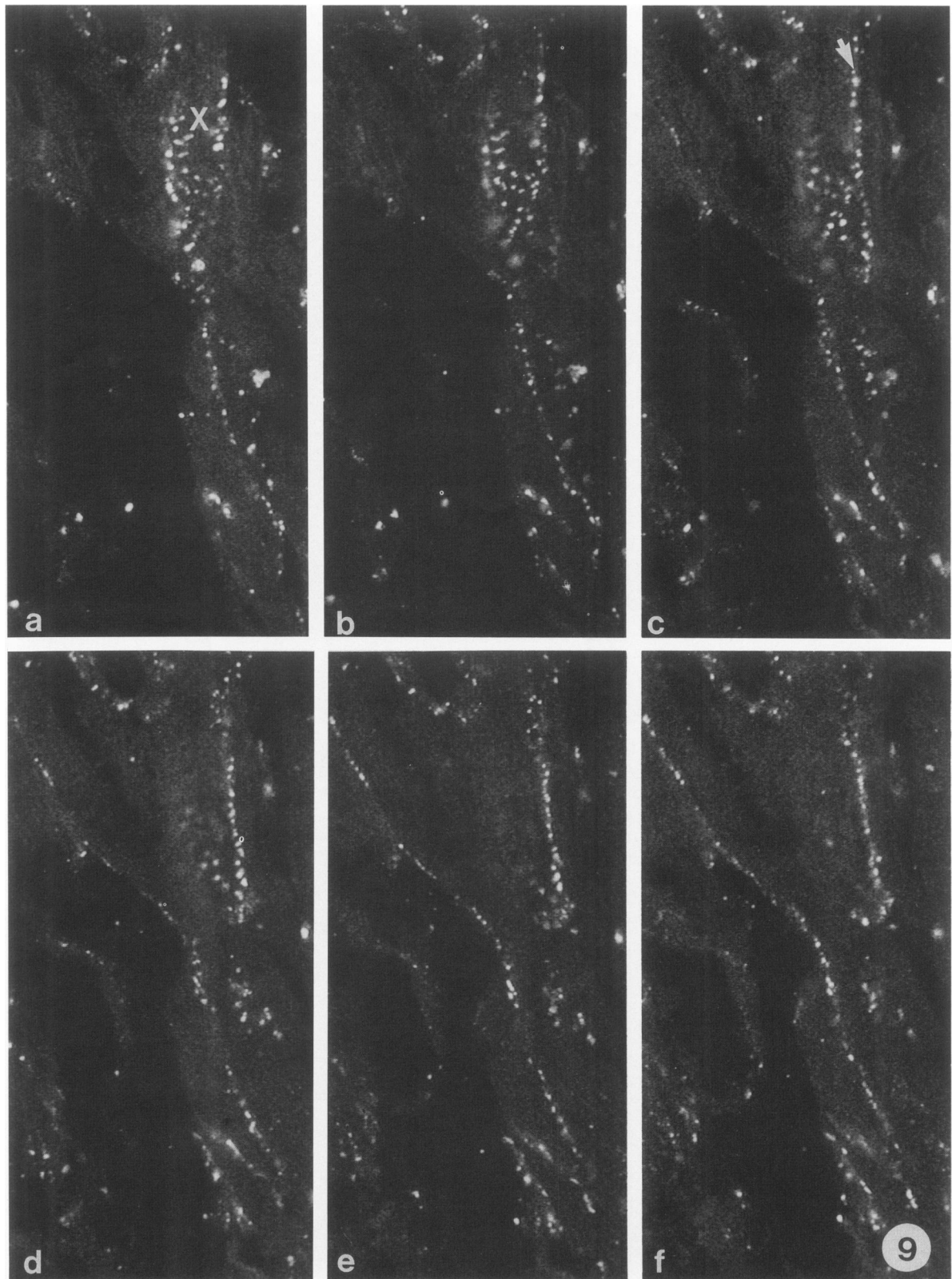


Figure 9. A series of optical sections (a–f) taken at 1 μm steps to examine the three-dimensional distribution of immunostained gap junctions in border zone myocytes (left ventricle, transplant patient). In the first view of the series (a), a group of immunostained gap junctions (*) is visible, extending in a line to the bottom right of the field. Taking this view alone, it is unclear whether the group of spots (*) is situated inside the cell or at its surface. This point is clarified, however, by the sequence of optical sections that follow (b–f). Inspection of the views in (a), (b), and (c) shows an overall general correspondence in staining pattern, but at the same time, some spots in the group disappear, while others come into view. By step (c), a string of spots (arrow) is seen extending to the top right. The simplest interpretation of these images is that the group of immunostained junctions (*) is associated with an area of the cell surface that is viewed essentially face-on in (a) and (b), but curves downwards over to the right, giving an edge-on view where the string of spots (arrow) come into view in (c). The long lines of spots in (d–e) appear to mark out the lateral surfaces of cells. Through all these images, the staining appears to be associated with the cell surface rather than deep within the cell interior, but it cannot be established with certainty whether the staining is localized actually on the cell surface, or whether it lies close to it, just below the surface, $\times 780$.

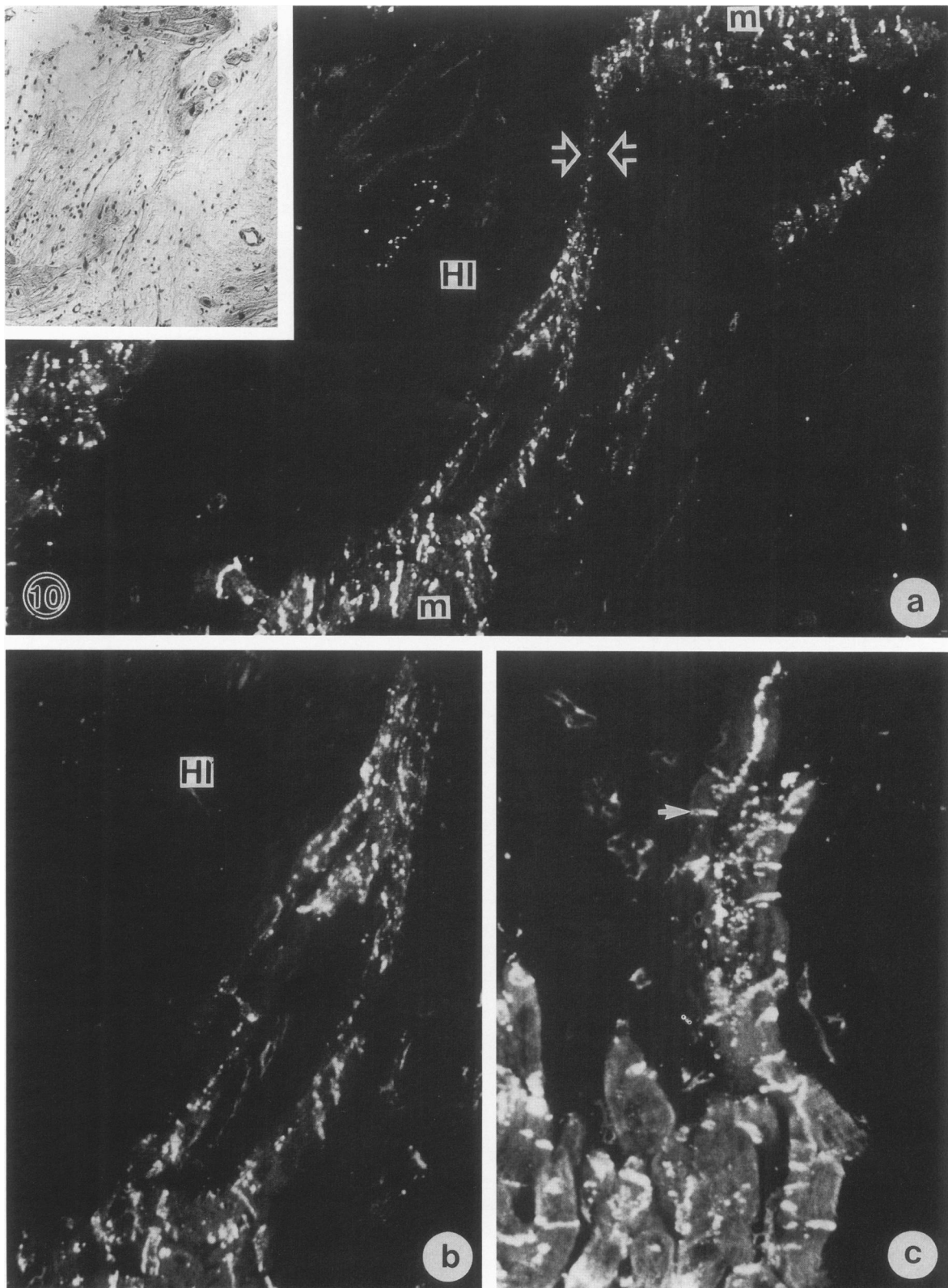


Figure 10. (a) shows in survey view a chain of myocytes, linked by immunolabeled gap junctions, crossing an extensive infarct zone (left ventricle, transplant patient). The thinnest part of the chain comprises the width of a single myocyte (between paired arrows). The "bridge" joins with myocardium (m) showing apparently normal intercalated disks on either side (M). The inset shows a view of the area to the top right of the field, as seen by conventional H & E histology of an adjacent section; (b) shows a higher magnification view of part of (a). In this, and in the example in (c) the distribution of labeled gap junctions is seen to become progressively more disorderly as the myocardial bridge penetrates into the infarct zone. In (b) typical disks are seen only at the base of a bridge; in (c) both typical disks (arrow) and dispersed junctions are apparent at the tip of a "peninsula." Composite images from multiple optical sections, a, $\times 156$; inset $\times 85$; b, $\times 270$; c, $\times 925$.

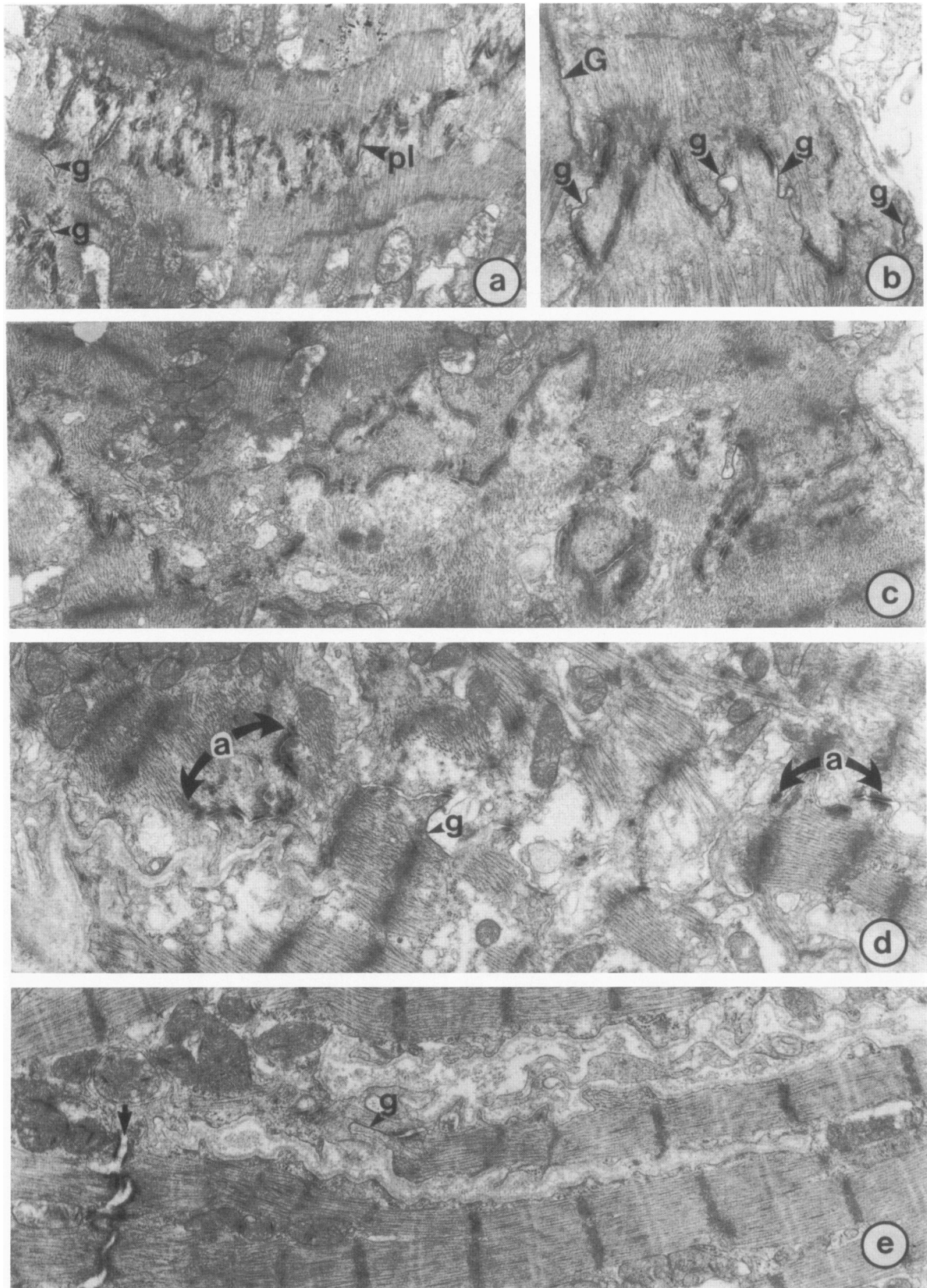


Figure 11. Thin-section electron microscopy survey views of intercalated disk morphology in infarct zone myocytes (left ventricle, needle biopsy); (a) cells that have well-preserved contractile apparatus show disk features similar to those of normal myocytes. The plicate region (pl) containing the fasciae adherentes is evenly folded, following a transverse path across the myofiber axis. Gap-junctional membrane (g) occurs in longitudinally oriented segments. b: In disks of normal appearance, the larger gap junctions often occur close to the periphery of the disk (G); smaller gap junctions (g) occur within the plicate zone, in association with fasciae adherentes. (c) example of a disk that has lost the regularity of folding characteristic of "normal" disks, between cells showing abnormalities in myofilament organization. An increased number of desmosomes, and a reduction in the numbers of gap junctions, are often apparent in disks with this morphology. d: Groups of junctions may become distanced apart as the disk loses its normal geometry and the overall morphology of the cells change. Note gap junction (g) at some distance from groups of adherens junctions (a). e: The membranes at some disks start to part (arrow), though in this example gap-junctional contact (g) is maintained at a distance location from the main disk. a, $\times 9400$; b, $\times 12400$; e, $\times 13600$; d, e, $\times 15300$.

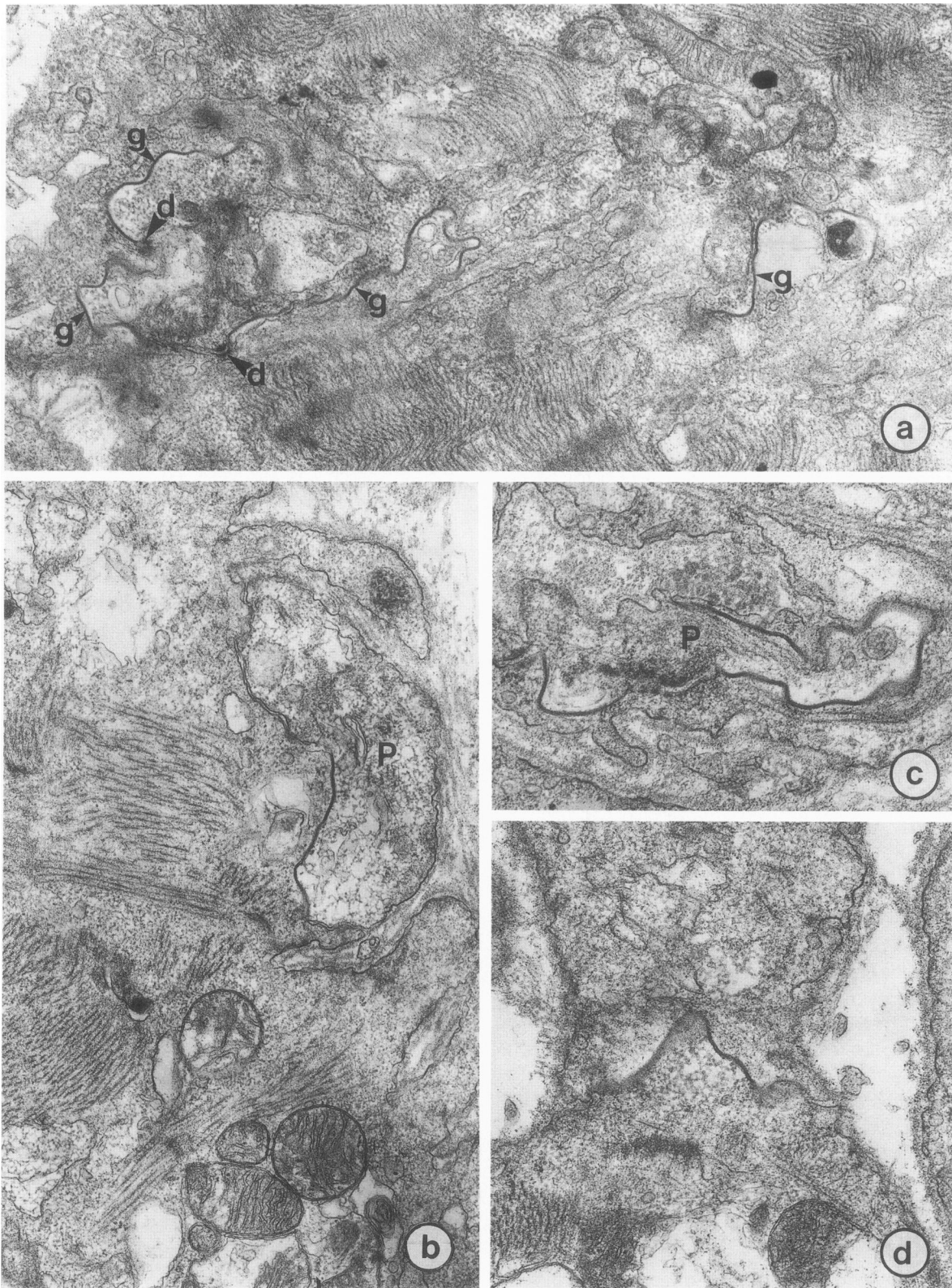


Figure 12. Examples of gap-junctional contact between myocytes in the absence of recognizable intercalated disks, as seen by thin-section electron microscopy of an infarct border zone from a needle biopsy (left ventricle); (a) shows a series of gap junctions (g), with two small desmosomes (d) but no other adherens junctions, between two degenerating myocytes that have an irregular surface topology and abnormal undulating myofilaments, (b, c) illustrate examples of similar interactions in which a cell process (P) of one cell is cross-sectioned at the point of gap-junctional contact with a neighboring cell. Note disorganized myofilaments in (b), (d) gap junction occupying almost the full extent of the blunt end of interacting cell processes, a, b, $\times 24500$; c, $\times 34500$; d, $\times 30500$.

volute profiles, are illustrated between cells with abnormally oriented myofilaments in Figure 12. Figure 12a shows a series of gap junctions, establishing contact in a region between two degenerating myocytes that is no longer recognizable as an intercalated disk. The surfaces of such cells are often ruffled with irregular cell processes that may form gap-junctional contacts at some distance from the main cell body (Figure 12b, c). Although in some section planes these junctions may present the appearance of having been internalized, single gap junctions occupying the end-on abutments of the cell processes can be demonstrated in appropriate section planes (Figure 12d).

Annular profiles of gap-junctional membrane are more abundant in infarct zone myocytes than in normal myocytes (Figure 13). The increased convolution of the junctional membranes in degenerating cells appears to be the main explanation for this phenomenon. However, in some instances (e.g., where isolated cytoplasmic adherent junctions are also observed), these structures may represent cytoplasmic vesicles of internalized gap-junctional membrane (Figure 13b). Occasional gap junctions attached to membrane blebs at the cell surface suggest disrupted junctional contacts that may be the precursors to such internalized vesicles (Figure 13c).

Discussion

By combining cardiac gap junction-specific antibody staining with laser scanning confocal microscopy, the present study has enabled visualization of gap junctions with exceptional clarity over extensive areas and through substantial depths of diseased human heart tissue. These unique images are achieved through the ability of the laser scanning confocal microscope to reduce out-of-focus blur, and to provide optical sections at variable levels through thick tissue slices.^{24,25} As a result, it has been possible 1) to define and compare some basic morphometric characteristics of myocardial gap junctions and intercalated disks in patients who have ischemic heart disease, 2) to establish that gap-junction distribution is characteristically altered in myocytes at the border zones of healed infarcts, and 3) to demonstrate the presence of myocyte bridges, coupled by gap junctions, extending across healed infarcts so as to link healthy myocardium on either side. The immunostaining procedure using "HJ", as applied in the present study, was specific for cardiac muscle cell gap junctions. The lack of specific immunostaining in vascular smooth muscle may be attributable to the small size of the connexin43-containing gap junctions, and the high level of autofluorescence, in these cells. Although valve myofibroblasts possess gap junctions, the nature of their com-

ponent connexins remains to be determined. Fibroblasts, even though capable of forming close associations with myocytes (e.g., in infarcts), do not appear to establish gap-junctional communication with them *in vivo*.

The overall patterns in the distribution of immunostained gap junctions observed in myocytes of well-preserved histologic structure accords with but also adds to the classical concepts of gap-junction organization at the cardiac intercalated disk derived from light microscopy, electron microscopy,^{4,6} and recent immunostaining results on nonhuman material examined by light microscopy after silver enhancement of signal.²⁶ Prominent ringlike arrangements of gap junctions at the periphery of the disk appear to be a feature common to a range of mammalian species examined with our antibody staining procedure and confocal microscopy.²³ In the patients who have advanced ischemic heart disease, left ventricular function was severely impaired whereas right ventricular function was well preserved. Our finding that in myocardium of essentially normal appearance histologically, there were no detectable differences between the two ventricles in apparent gap junction size, distribution, or in the number of junctions per unit area of disk suggests that a generalized, widespread derangement in gap junction organization does not underlie functional impairment in the ischemic heart. This conclusion appears to be reinforced by our finding of similar results in the myocardium of the patient who had primary pulmonary hypertension.

Arrhythmias, and in particular re-entry arrhythmias, are a prominent feature of ischemic heart disease.¹⁻³ In experimentally induced infarction, electrophysiologic studies have identified the border zone of myocardial infarcts as sites in which slow conduction, responsible for sustained re-entry, arises.²⁷⁻²⁹ Slow conduction, attributable to intercellular uncoupling, and areas of complete conduction block, persist at the sites of experimentally induced infarction after healing, thereby contributing to chronic arrhythmogenesis.²⁷⁻²⁹ Ultrastructurally, examination of the intercalated disks in border zone-myocytes after experimental ischemia reveals attenuation of "contact zones,"²⁹ and in human ischemic heart disease, a reduction in the size and density of gap junctions in these cells has recently been briefly reported.³⁰

We have shown, with the new overviews of gap-junction distribution afforded by antibody labeling and laser scanning confocal microscopy, that the most prominent and consistent feature of border zone myocytes in human ischemic heart disease, is a disorderly pattern of stained gap junctions. Comparatively few labeled gap junctions are organized in discrete intercalated disks, and many are spread laterally over the cell. It is tempting to suggest that such a derangement might contribute to re-entry arrhythmias by altering the normal conduction

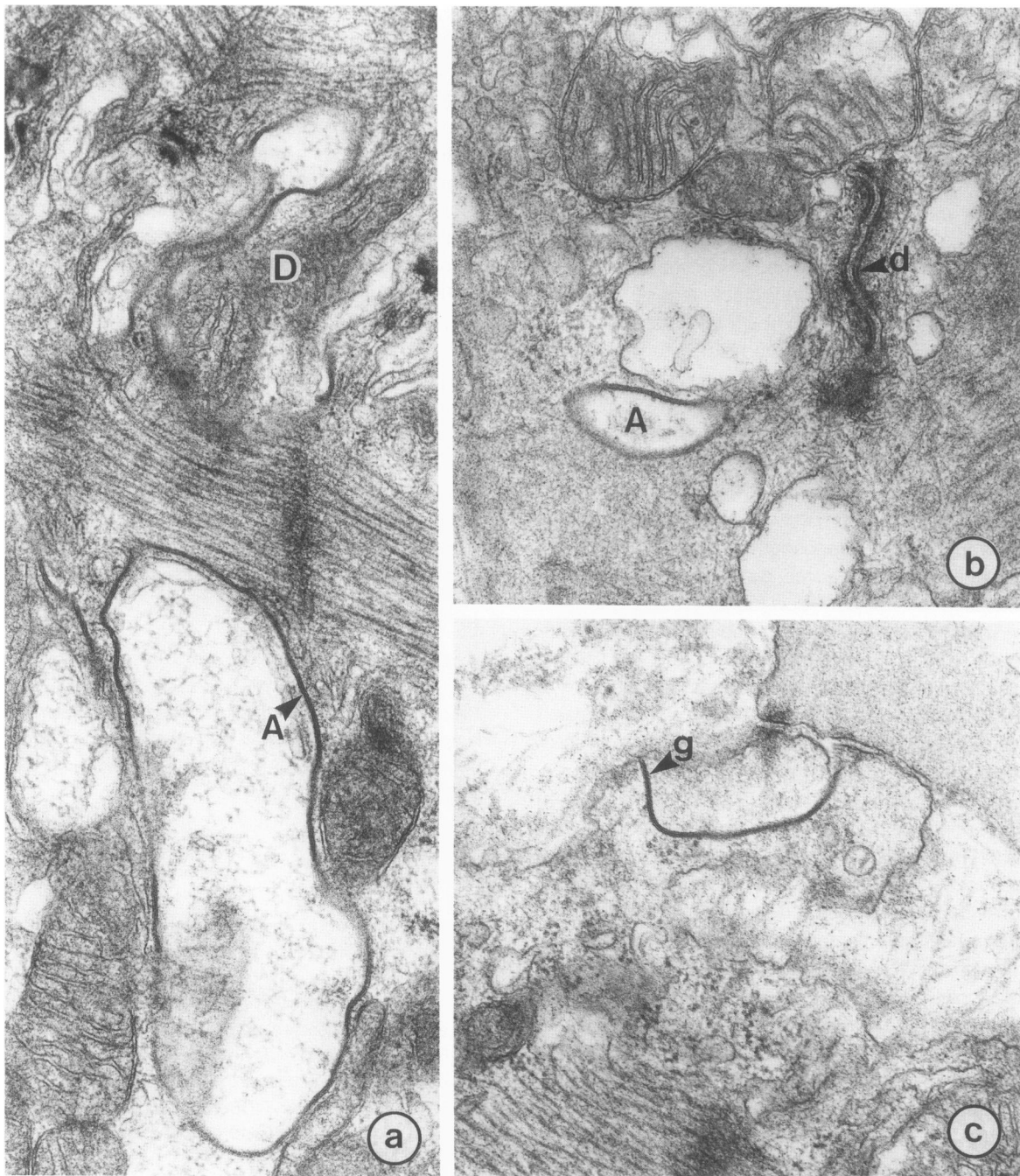


Figure 13. Annular profiles of gap-junctional membrane observed in border-zone myocytes by thin-section electron microscopy; (a) shows a large annular profile (A), which because of its proximity to an (abnormal) intercalated disk (D), probably represents a highly convoluted junction attached to the disk; (b) shows a smaller annular profile (A), and an isolated desmosome (d), which appear to have been internalized; (c) surface-located gap junction (g) attached to a membrane bleb, possibly representing a disrupted (nonfunctional) junction. a, $\times 46800$; b, $\times 45000$; c, $\times 49500$.

properties between myocytes. The velocity of impulse conduction appears to be affected by myocyte orientation, myocardial conduction parallel to the long axis of the cells being more rapid than that transversely,^{27,31} and this effect is presumably mediated at least in part by the pattern of gap-junction arrangement. The possibility thus

exists that injury-induced disruption of the normal gap arrangement could play a direct role in arrhythmogenesis.

Other factors that could conceivably interfere with normal conduction include alterations in the channel properties of individual junctions, and diminution in the quantity of functional gap junction membrane. As our antibod-

ies are directed to gap-junctional protein,^{19,20} the presence of positive staining should be interpreted strictly as the presence of this protein, and is not necessarily a marker for the fully functional gap junction. Disassembly of gap junctions, at least in some systems, may involve separation of the once-abutting connexons of adjacent membranes, and their lateral dispersion in the plasma membrane.^{32,33} We cannot exclude, therefore, that the lateral staining found in border zone myocytes may at least in part be due to gap junction disassembly. A second mechanism by which cells remove unwanted gap-junctional membrane is by internalization.³⁴ When myocytes are forcibly separated experimentally, for example, large numbers of gap junctions are pinched-off into the cell by endocytosis, producing cytoplasmic vesicles of gap-junctional membrane which may persist, just below the cell surface, for substantial periods.³⁵ Although serial optical sections revealed that some of the dispersed patches of immunostaining were located in the vicinity of cell-to-cell appositions, the technique does not have the resolution required to determine whether these structures lie on or just below the cell surface.

Thin-section electron microscopy provided further insight into these issues by revealing multiple and variable alterations to the intercalated disk and gap junctions of border zone myocytes. Myocytes in the vicinity of healed infarcts undergo diverse alterations in morphology, associated with a remodelling of their intercellular interactions. Individual junctions and groups of junctions, though often maintaining intercellular contact, appear to be displaced by this remodelling process, so that discrete intercalated disk zones are, overall, less clearly defined. Some junctional contacts are entirely disrupted by these changes, leaving junctional membrane associated with blebs at the cell surface, or internalized just below the surface as intracytoplasmic structures. Both gap junctions and adherentes junctions are affected by these processes. Intracytoplasmic junctions (mainly adherentes junctions but also gap junctions) have previously been reported as a feature of degenerating myocytes associated with areas of fibrosis in a variety of cardiac pathologic conditions.³⁶ Both displaced gap junctions that maintain contact between cells, and internalized, nonfunctional, gap-junctional membrane, are likely to contribute to the dispersed immunostaining pattern observed by confocal microscopy. However, although electron microscopy can reveal the fine detail of the ultrastructural location of individual segments of junctional membrane, it is only by confocal microscopy of immunostained preparations that the full extent of the reorganization in the distribution of gap-junctional membrane in the tissue as a whole becomes apparent.

The presence of myocytic strands traversing some infarcts suggests a means by which any potential elec-

trophysiologic disruption associated with these zones may be minimized or avoided. Similar peninsulas into and bridges across infarcted regions have been previously reported in histologic studies.³⁷ The present study, by showing that gap-junctional staining between myocytes is continuous across such strands, demonstrates that potentially at least, the component cells are electrically coupled. Even if there is an altered gap-junction distribution in some of the myocytes making up the strands, and this has some effect on conduction velocity, such structures could nevertheless form electrically coupled bridges across what might otherwise constitute blocked zones, thereby encouraging uninterrupted transmission of the impulse between areas of healthy myocardium. The impression is, however, that if such a situation exists, it may lie in precarious balance, for the thinnest part of some bridges is no wider than a single myocyte. The continued survival of the myocytes making up these bridges may therefore be important for maintenance of a stable electrophysiologic state in ischemic heart disease.

Acknowledgments

The authors thank Drs. S. Harding, F. Del Monte, J. Mann, and the surgical staff at Harefield, the Royal Brompton, and St. George's Hospitals for their help in providing specimens of diseased human heart.

References

1. Adgey AAJ: Acute phase of ischemic heart disease and myocardial infarction. Boston, Martinus Nijhoff, 1982, 201
2. Kleber AG: Review. Conduction of the impulse in the ischemic myocardium—implications for malignant ventricular arrhythmias. *Experientia* 1987, 43:1056–1061
3. Hoffman BF, Dangman KH: Review. Mechanisms for cardiac arrhythmias. *Experientia* 1987, 43:1049–1056
4. Forbes MS, Sperelakis N: Intercalated discs of mammalian heart: a review of structure and function. *Tiss Cell* 1985, 17:605–648
5. Page E, Manjunath CK: Communicating junctions between heart cells. *The Heart and Cardiovascular System*, vol 1. Edited by HA Fozzard, E Haber, RB Jennings, AM Katz, HE Morgan. New York, Raven Press, 1986, pp 573–600
6. Severs NJ: The cardiac gap junction and intercalated disc. *Intl J Cardiol* 1990, 26:137–173
7. Warner AE: The gap junction. *J Cell Sci* 1988, 89:1–7
8. Green CR: Evidence mounts for the role of gap junctions during development. *BioEssays* 1988, 8:7–10
9. Zimmer DB, Green CR, Evans WH, Gilula NB: Topological analysis of the major protein in isolated intact rat liver gap junctions and gap junction-derived single membrane structures. *J Biol Chem* 1987, 262:7751–7763

10. Milks LC, Kumar NM, Houghten R, Unwin N, Gilula NB: Topology of the 32-kD liver gap junction protein determined by site-directed antibody localizations. *EMBO J* 1988, 7:2967–2975
11. Paul DL: Molecular cloning of cDNA for rat liver gap junction protein. *J Cell Biol* 1986, 103:123–134
12. Kumar NM, Gilula NB: Cloning and characterization of human and rat liver cDNAs coding for a gap junction protein. *J Cell Biol* 1986, 103:767–776
13. Zhang J-T, Nicholson B: Sequence and tissue distribution of a second protein of hepatic gap junctions, C × 26, as deduced from its cDNA. *J Cell Biol* 1989, 109:3391–3401
14. Kistler J, Christie D, Bullivant S: Homologies between gap junction proteins in lens, heart and liver. *Nature* 1988, 331, 721–723
15. Gimlich RL, Kumar NM, Gilula NB: Sequence and developmental expression of mRNA coding for a gap junction protein in *Xenopus*. *J Cell Biol* 1988, 107:1065–1073
16. Ebihara L, Beyer EC, Swenson KI, Paul DL, Goodenough DA: Cloning and expression of a *Xenopus* embryonic gap junction protein. *Science* 1989, 243:1194–1195
17. Beyer EC, Paul DL, Goodenough DA: Connexin43: a protein from rat heart homologous to a gap junction protein from liver. *J Cell Biol* 1987, 105:2621–2629
18. Yancey SB, John SA, Lal R, Austin BJ, Revel J-P: The 43-kD polypeptide of heart gap junctions: immunolocalization, topology and functional domains. *J Cell Biol* 1989, 108:2241–2254
19. Gourdie RG, Harfst E, Severs NJ, Green CR: Cardiac gap junctions in rat ventricle: localization using site directed antibodies and laser scanning confocal microscopy. *Cardioscience* 1990, 1:75–82
20. Harfst E, Severs NJ, Green CR: Cardiac myocyte gap junctions: evidence for a major connexon protein with an apparent relative molecular mass of 70 000. *J Cell Sci* 1990, 96:591–604
21. Toshimori H, Toshimori K, Oura C, Matsuo H: Immunohistochemistry and immunocytochemistry of natriuretic peptide in porcine heart. *Histochemistry* 1987, 86:595–601
22. Harlow E, Lane D: *Antibodies: A laboratory manual*. Cold Spring Harbor, Cold Spring Harbor Laboratory, 1988
23. Gourdie RG, Green CR, Severs NJ: Gap junction distribution in adult mammalian myocardium revealed by an antipeptide antibody and laser scanning confocal microscopy. *J Cell Sci* 1991, 99:41–55
24. White JG, Amos WB, Fordham M: An evaluation of confocal versus conventional imaging of biological structure by fluorescence light microscopy. *J Cell Biol* 1987, 105:41–48
25. Shotton DM: Review. Confocal scanning optical microscopy and its applications for biological specimens. *J Cell Sci* 1989, 94:175–206
26. Luke RA, Beyer EC, Hoyt RH, Saffitz JE: Quantitative analysis of intercellular connections by immunohistochemistry of the cardiac gap junction protein connexin43. *Circ Res* 1989, 65:1450–1457
27. Spear JF, Michelson EL, Moore EN: Cellular electrophysiologic characteristics of chronically infarcted myocardium in dogs susceptible to sustained ventricular tachyarrhythmias. *J Am Coll Cardiol* 1983, 1:1099–1110
28. Dillon SM, Allesie MA, Ursell PC, Wit AL: Influences of anisotropic tissue structure on reentrant circuits in the epicardial border zone of subacute canine infarcts. *Circ Res* 1988, 63:182–206
29. Ursell PC, Gardner PI, Albala A, Fenoglio JJ, Wit AL: Structural and electrophysiological changes in the epicardial border zone of canine myocardial infarcts during infarct healing. *Circ Res* 1985, 56:436–451
30. Luke RA, Hoyt RH, Tolley TK, Saffitz JE: Altered myocyte gap junction distribution in regions bordering healed infarcts. *Circulation* 1989, 80:II–499
31. Whittaker P, Boughner DR, Kloner RA: Analysis of healing after myocardial infarction using polarized light microscopy. *Am J Pathol* 1989, 134:879–893
32. Lane NJ, Swales LS: Dispersal of gap-junctional particles, not internalization, during the in vivo disappearance of gap junctions. *Cell* 1980, 19:579–586
33. Braun J, Abney JR, Owlicki JC: How a gap junction maintains its structure. *Nature* 1984, 310:316–318
34. Larsen WJ, Risinger MA: The dynamic life histories of intercellular membrane junctions. *Modern Cell Biology* 1985, 4:151–216
35. Severs NJ, Shovel KS, Slade AM, Powell T, Twist VW, Green CR: Fate of gap junctions in isolated adult mammalian cardiomyocytes. *Circ Res* 1989, 65:22–42
36. Buja LM, Ferrans VJ, Maron BJ: Intracytoplasmic junctions in cardiac muscle cells. *Am J Pathol* 1974, 74:613–648
37. Factor SM, Sonnenblick EH, Kirk ES: The histologic border zone of acute myocardial infarction—'islands' or 'peninsulas'? *Am J Pathol* 1978, 92:111–124